2018 European Control Conference (ECC)
June 12-15, 2018. Limassol, Cyprus

Receding horizon heat flow control in domestic buildings - Yesterday-based disturbance predictions*

Yannik Löhr[1] and Martin Mönnigmann[1]

***Abstract*— We design and investigate a receding horizon control method for heat generation, storage and consumption in domestic buildings. The approach allows the controller to use storage capacities and comfort windows to react on varying external conditions and forecasts, including weather or time-dependent energy tariffs. We demonstrate it is efficient to optimize heat generation and distribution simultaneously. The controller shows a good performance when perfect forecasts are assumed. The performance decreases only slightly, if historical data is chosen as forecast for the upcoming day. In particular, the controller still operates the system within the predefined comfort windows most of the time and the heat consumption and heat generation costs increase only mildly.**

I. Introduction

Heating, ventilation and air conditioning (HVAC) of residential buildings accounts for a significant amount of the building energy consumption [1]. In wide parts of Europe, heating is the main contributor to energy demand of HVAC systems. Among other things, stricter regulations have resulted in more complex heating systems, which today feature different means of heat generation and storages in single buildings. Recently, a common setup for heating systems is the combination of thermal energy storage with heat pump or solar heat generation. An example is given in [2], where a net zero energy building with on-site thermal energy generation and storage is investigated.

Optimal control methods are an intuitive choice for handling increasing complexity. Wang et al. found that about one third of scientific publications on control of HVAC systems during the last ten years investigate model predictive control (MPC) methods [3]. Approaches for modeling of buildings include black-box models or RC-network equivalent models [4]. Furthermore, it is established to derive more detailed models with software such as EnergyPlus [5] and to adapt them for control design [6],[7].

There are several approaches for the design of MPC in building control. A common objective is the minimization of the energy consumption or cost, while the controller has to guarantee the occupants' comfort. In [7] for example, the authors introduce a weighting factor to achieve a trade-off between these two competing objectives. Other work indicates the usefulness of economic MPC, especially in the context of a smart grid [8]. The importance of accurate disturbance information has also been investigated. Oldewurtel et al. demonstrated potential energy savings if occupancy information is used in HVAC control in office buildings [9]. In [10], the authors introduced a robust MPC approach to handle uncertainties in model and disturbance predictions.

In this work, we generalize a heating system similar to [11], use a building model based on EnergyPlus [5] and design an optimal control task for heat generation, storage and consumption. Due to continuously changing external and internal conditions and differing comfort requirements between day and night, the system environment is time-variant. We further analyze the control performance if the data from a previous day is used to predict the upcoming day's disturbances.

In Section II, we derive a model of the considered heating system. Then, we formulate an optimal control task in Section III by posing suitable costs and constraints. Sections IV and V present results from an extensive simulation study.

II. Heating system

In this study, we design and apply a discrete-time receding horizon controller for combined domestic heat generation, distribution and consumption. The system is shown in Fig. 1. It consists of a generation and a consumption subsystem, which will be introduced in Section II-A and Section II-B, respectively.

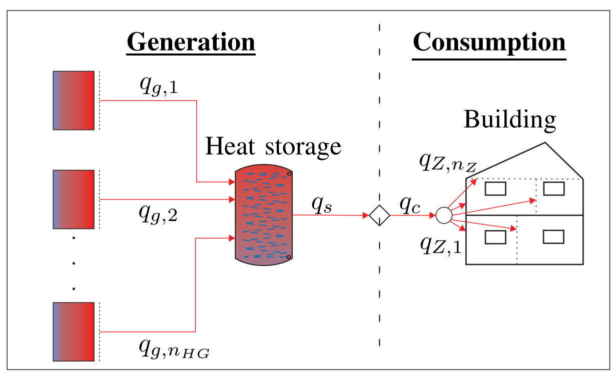

Fig. 1: Structure of heat generation and consumption system

A. Generation system

The system for heat generation is an adaption of the one introduced in [11]. We consider a number n_{HG} of heat generators with different efficiencies and operation ranges. The generated heat flows are denoted by $q_{g,i}(k), i = 1, 2, \dots, n_{HG}$, where $k = 0, 1, \dots$ enumerates time steps. The system also includes a heat storage. We accomplish heat supply to the consumption subsystem by discharging the storage with heat flow $q_s(k)$ exclusively. In other words,

*This work was supported by the German Federal Ministry of Economic Affairs and Energy under grant 03ET1274B.

[1]Yannik Löhr and Martin Mönnigmann are with Department of Mechanical Engineering, Automatic Control and Systems Theory, Ruhr-University Bochum, Bochum, Germany (yannik.loehr@rub.de, martin.moennigmann@rub.de)

978-3-9524-2699-9 ©2018 EUCA

there exists only a single physical connection between the generation and consumption system through the heat storage (see Fig. 1). The detailed dynamics of the components can be neglected, since they are fast compared to the sampling time. In particular, the heat flows are considered to be static quantities, since their dynamics are fast compared to the high thermal inertia of the storage. As a consequence, we may model heat generation and supply by time-dependent restrictions, i.e.

$$0 \leq q_{g,i}(k) \leq q_{g,i}^{\max}(k),\ i = 1, \ldots, n_{HG}, \tag{1a}$$

$$0 \leq q_s(k) \ \leq q_s^{\max}(k), \tag{1b}$$

for given $q_{g,i}^{\max}(k)$ and $q_s^{\max}(k)$. The rates of change of $q_{g,i}(k)$, modeled by $q_{g,i}(k+1) - q_{g,i}(k)$, are also subject to constraints

$$-\dot{q}_{g,i}^{\min} \leq q_{g,i}(k+1) - q_{g,i}(k) \leq \dot{q}_{g,i}^{\max},\ i = 1, \ldots, n_{HG}, \tag{2a}$$

$$-\dot{q}_s^{\min} \leq q_s(k+1) - q_s(k) \quad \leq \dot{q}_s^{\max}, \tag{2b}$$

for all k and for given $\dot{q}_{g,i}^{\min}$, $\dot{q}_{g,i}^{\max}$, $\dot{q}_s^{\min}$ and $\dot{q}_s^{\max}$. The stored heat $E_{\text{th}}(k)$ is subject to the bounds

$$E_{\text{th}}^{\min} \leq E_{\text{th}}(k) \leq E_{\text{th}}^{\max} \tag{3}$$

and described by the simplified energy balance

$$E_{\text{th}}(k+1) = \alpha E_{\text{th}}(k) - \beta_s q_s(k) + \textstyle\sum_{i=1}^{n_{HG}} \beta_i q_{g,i}(k), \tag{4}$$

where $\alpha \leq 1, \beta_i \leq 1, i = s, 1, 2, .., n_{HG}$ represent storage losses and discharging and charging efficiencies, respectively. We understand (4) as dynamics of the generation system with state $E_{\text{th}}(k)$ and inputs $\mu(k) = [q_s(k), q_{g,1}(k), q_{g,2}(k), \ldots, q_{g,n_{HG}}(k)]^T \in \mathbb{R}^{n_{HG}+1}$.

B. Consumption system

We consider a domestic building that is divided into n_Z zones. The temperatures of these zones and of the $(n_\xi - n_Z)$ remaining construction elements (e.g. walls, surfaces) are stored as states $\xi(k) = [T_{Z,1}, \ldots, T_{Z,n_Z}, \ldots]^T \in \mathbb{R}^{n_\xi}$. We regard the heat flows $\nu(k) = [q_{Z,1}, q_{Z,2}, ...]^T \in \mathbb{R}^{m_\xi}$ as inputs into the heated zones, which implies $m_\xi \leq n_Z$. Measured disturbances $\zeta(k) \in \mathbb{R}^{l_\xi}$ comprise ambient weather conditions and internal gains, where the latter comprise heat emitted by occupants and electrical appliances. The building model reads

$$\xi(k+1) = \mathbf{A}_\xi \xi(k) + \mathbf{B}_\xi \nu(k) + \mathbf{E}_\xi \zeta(k). \tag{5}$$

Further information on the matrices in (5) will be given in Sec. IV. The heat flows into each of the zones are bounded by

$$0 \leq q_{Z,i}(k) \leq q_{Z,i}^{\max}(k), i = 1, 2, \ldots, m_\xi. \tag{6}$$

Similarly to (2), the rates of change of $q_{Z,i}(k)$ are subject to constraints

$$-\dot{q}_{Z,i}^{\min} \leq q_{Z,i}(k+1) - q_{Z,i}(k) \leq \dot{q}_{Z,i}^{\max},\ i = 1, 2, ..., m_\xi, \tag{7}$$

for given bounds $\dot{q}_{Z,i}^{\min}$ and $\dot{q}_{Z,i}^{\max}$.

C. Combination of heat generation and consumption

Collecting (4) and (5) results in the state space model

$$\mathbf{x}(k+1) = \mathbf{A}\mathbf{x}(k) + \mathbf{B}\mathbf{u}(k) + \mathbf{E}\mathbf{d}(k), \tag{8}$$

with states $\mathbf{x}(k) = [E_{\text{th}}(k), \xi(k)]^T \in \mathbb{R}^n$, inputs $\mathbf{u}(k) = [\mu(k), \nu(k)]^T \in \mathbb{R}^m$, measured disturbances $\mathbf{d}(k) = [\zeta(k)]^T \in \mathbb{R}^l$ and system matrices

$$\mathbf{A} = \begin{bmatrix} \alpha & \underline{\mathbf{0}} \\ \underline{\mathbf{0}} & \mathbf{A}_\xi \end{bmatrix}, \mathbf{B} = \begin{bmatrix} \begin{bmatrix} -\beta_s & \beta_1 & \ldots & \beta_{n_{HG}} \end{bmatrix} & \underline{\mathbf{0}} \\ \underline{\mathbf{0}} & \mathbf{B}_\xi \end{bmatrix}$$

and $\mathbf{E} = [\underline{\mathbf{0}},\ \mathbf{E}_\xi]^T$, where $\underline{\mathbf{0}}$ are zero matrices of suitable dimensions.

III. Control design

The controller needs to satisfy two goals. Most importantly, it must guarantee the occupants' thermal comfort. Secondly, the system must be operated economically. We achieve the desirable behavior by a suitable design of the optimal control task, i.e. the proper choice of constraints and cost function. The temperatures of the occupied zones must be kept within certain comfort windows. Since these windows are different for days than for nights, time-dependent constraints result. In addition, we penalize deviations from temperature set points for temperatures for the occupied zones whenever they are actually occupied. This, among other terms, leads to a time-dependent cost function. The constraints and cost function are also time-dependent, since energy costs are functions of time. Note that the combination of comfort windows and the various time-dependencies implies that cost optimal operation is not equivalent to operation for minimal energy consumption. In specific periods, large price differences can make it economically preferable to generate more heat than needed, for example.

A. Cost function

Let $q_j(k+i|k)$, $T_{Z,j}(k+i|k)$ etc. refer to the predicted values of q_j, $T_{Z,j}$ etc. for time $k+i$ based on the information available at time k. We define the index set

$$\boldsymbol{\mathcal{L}} = \{l | l \in \{(s), (g, j_{HG}), (Z, j), (set, j)\}\}, \tag{9}$$

where $j_{HG} = 1, 2, .., n_{HG}$ and $j = 1, .., m_\xi$ to simplify the notation. In (9), the indices s and g, j_{HG} refer to the quantities of the generation system introduced in Section II-A and the indices Z, j and set, j refer to the quantities of the consumption system introduced in Section II-B. The cost function penalizes the heat flows in the system and the deviation of set points with scalar costs $c_l(k+i)$, $l \in \boldsymbol{\mathcal{L}}$. Specifically,

$$J_s(k) = \textstyle\sum_{i=0}^{N-1} c_s(k+i)\left(q_s(k+i|k)\right)^2, \tag{10a}$$

$$J_g(k) = \textstyle\sum_{j=1}^{n_{HG}} \sum_{i=0}^{N-1} c_{g,j}(k+i)(q_{g,j}(k+i|k))^2, \tag{10b}$$

$$J_Z(k) = \textstyle\sum_{j=1}^{m_\xi} \sum_{i=0}^{N-1} c_{Z,j}(k+i)(q_{Z,j}(k+i|k))^2, \tag{10c}$$

penalize the discharging heat flow, the generated heat flows and the heat flows into each of the thermal zones, respectively, where N denotes the horizon. Set-point tracking is enforced for up to n_Z building zones by adding

$$J_{set}(k) = \textstyle\sum_{j=1}^{n_Z} \sum_{i=0}^{N-1} c_{set,j}(k+i)\left(T_{Z,j}(k+i|k) - T_{Z,j}^{set}(k+i)\right)^2, \tag{11}$$

for given time-variant set points $T_{Z,j}^{set}(k+i)$. Additionally, we denote input actions by $\Delta\mathbf{u}$ and penalize rapid input changes with

$$J_{\Delta u}(k) = \textstyle\sum_{i=0}^{N-1} \mathbf{c}_{\Delta u}(\Delta\mathbf{u}(k+i|k))^2. \tag{12}$$

Let us define the controlled outputs as

$$\mathbf{z}(k) = \begin{bmatrix} \mathbf{C}_z & \underline{\mathbf{0}} \\ \underline{\mathbf{0}} & \underline{\mathbf{0}} \end{bmatrix} \mathbf{x}(k) + \begin{bmatrix} \underline{\mathbf{0}} & \underline{\mathbf{0}} \\ \underline{\mathbf{0}} & \mathbf{1}_m \end{bmatrix} \mathbf{u}(k), \tag{13}$$

where $\mathbf{C}_z$ relates to measurable outputs, i.e. the zone temperatures, and $\mathbf{1}_m \in \mathbb{R}^{m\times m}$ is a unit matrix. We further define a reference vector $\mathbf{r}(k) = [T^{set}_{Z,1}(k), \dots, T^{set}_{Z,n_Z}(k), \mathbf{0}_m]^T \in \mathbb{R}^{nz+m}$ and denote the the control error by $\mathbf{e}(k) = \mathbf{r}(k) - \mathbf{z}(k)$. The sum of (10)-(12) can then be written as

$$J(k) = \sum_{i=0}^{N-1} \|\mathbf{e}(k+i|k)\|^2_{\boldsymbol{\mathcal{Q}}(k+i)} + \sum_{i=0}^{N-1} \|\Delta\mathbf{u}(k+i|k)\|^2_{\boldsymbol{\mathcal{R}}}, \tag{14}$$

where $\boldsymbol{\mathcal{Q}}(k+i) \geq 0$ and $\boldsymbol{\mathcal{R}} > 0$ are matrices containing the scalar costs. We denote the series of optimal input actions by $\Delta\mathbf{U}(k) = [\Delta\mathbf{u}(k|k), \Delta\mathbf{u}(k+1|k), \dots, \Delta\mathbf{u}(k+N-1|k)]^T$. Furthermore, let $\boldsymbol{\mathcal{E}}(k)$, $\boldsymbol{\mathcal{Q}}_q(k)$ and $\boldsymbol{\mathcal{R}}_q(k)$ incorporate the evolution of $\mathbf{e}(k)$, $\boldsymbol{\mathcal{Q}}(k)$ and $\boldsymbol{\mathcal{R}}$ along N, respectively. Applying these definitions, we can write (14) in compact form

$$J(k) = \|\boldsymbol{\mathcal{E}}(k)\|^2_{\boldsymbol{\mathcal{Q}}_q(k)} + \|\Delta\mathbf{U}(k)\|^2_{\boldsymbol{\mathcal{R}}_q(k)}. \tag{15}$$

B. Constraints

The link between the two subsystems can conveniently be established with an equality constraint. The constraint

$$q_s(k) = \frac{1}{\gamma}\sum_{i=1}^{m_\xi} q_{Z,i}(k), \tag{16}$$

where $\gamma \leq 1$ models heat transmission losses, ensures that the heat flow supplied by generation subsystem always matches the sum of heat flows required by the consumption subsystem. We transform (16) into two inequality constraints and combine them with the time-varying constraints (1) and (6) to

$$\boldsymbol{\mathcal{G}}\mathbf{u}(k) \leq \mathbf{g}(k), \tag{17}$$

where

$$\boldsymbol{\mathcal{G}} = \begin{bmatrix} \mathbf{1}_{+-} & \underline{\mathbf{0}} & \mathbf{0}_2 \\ & & \\ \mathbf{0}_2 & \ddots & \mathbf{0}_2 \\ \mathbf{0}_2 & \underline{\mathbf{0}} & \mathbf{1}_{+-} \\ \gamma & \mathbf{0}_{n_{HG}} & -\mathbf{1}_{m_\xi} \\ -\gamma & \mathbf{0}_{n_{HG}} & \mathbf{1}_{m_\xi} \end{bmatrix} \text{ and } \mathbf{g}(k) = \begin{bmatrix} q_s^{\max}(k) \\ 0 \\ q_{g,1}^{\max}(k) \\ 0 \\ \vdots \\ q_{i,m_\xi}^{\max}(k) \\ 0 \\ 0 \\ 0 \end{bmatrix}, \tag{18}$$

with $\mathbf{1}_{+-} = [1, \ -1]^T$ and $\mathbf{0}_2 = [0, \ 0]^T$. Furthermore, we require the zone temperatures to meet given comfort bounds

$$T^{\min}_{Z,j}(k) \leq T_{Z,j}(k) \leq T^{\max}_{Z,j}(k), j = 1, \dots, n_Z. \tag{19}$$

Using the dynamics (8) and applying the transformations shown in [12, pp.81-83] and [11], the constraints (17), the state constraints (19), (3), and the time-invariant box constraints (2), (7) on the input rates can be enforced over the N steps of the prediction horizon, and stated in terms of the input rates $\Delta\mathbf{U}(k)$. This results in constraints of the form

$$\boldsymbol{\Omega}\Delta\mathbf{U}(k) \leq \boldsymbol{\omega}(k). \tag{20}$$

C. Simple norm-based robust receding horizon control

Since the predictions of the ambient conditions and the internal gains are subject to uncertainty, we need to take measures to ensure feasibility. We introduce a slack variable $\epsilon(k)$ to soften the constraints on the zone temperatures (19) and add the penalty $J_\epsilon = \sum_{i=0}^{N-1} \mathbf{c}_\epsilon \epsilon(k+i)^2$ to the cost function (15). We then transform extended cost function and constraints (20) into a quadratic program

$$\min_{\boldsymbol{\Delta}\mathbf{U}(k),\epsilon(k)} \begin{bmatrix} \boldsymbol{\Delta}\mathbf{U}(k) \\ \epsilon(k) \end{bmatrix}^T \boldsymbol{\mathcal{H}}(k) \begin{bmatrix} \boldsymbol{\Delta}\mathbf{U}(k) \\ \epsilon(k) \end{bmatrix} - \boldsymbol{\mathcal{F}}^T(k) \begin{bmatrix} \boldsymbol{\Delta}\mathbf{U}(k) \\ \epsilon(k) \end{bmatrix} \tag{21}$$

$$\text{s.t. } \boldsymbol{\Omega}_\epsilon \begin{bmatrix} \boldsymbol{\Delta}\mathbf{U}(k) \\ \epsilon(k) \end{bmatrix} \leq \boldsymbol{\omega}_\epsilon(k).$$

The calculations that lead to (21) are lengthy but standard. We refer to [12, pp.74-77,83,98,147-148] and [13, pp.146-148] for further details and the recipes for the construction of the matrices in particular.

The optimal control problem is solved for every k, then the first element of the optimal inputs $\mathbf{U}^*(k) = \mathbf{U}(k-1) + \Delta\mathbf{U}^*(k)$ is applied to the system.

IV. Simulation study

A. Setup of heating system

We consider a heat generation system with one thermal storage and two heat generators, a variable speed heat pump generating $q_{g,1}(k)$ and a continuously controllable electrical heating element generating $q_{g,2}(k)$. Time-dependent restrictions on the generated heat apply as stated in Sec. II-A. The maximum heat pump power is linked to ambient conditions by a heat pump map [14], and it is assumed to be subject to blocking times as described in [11] (see Fig. 2 in [11] for an example). The storage is chosen to be sufficiently large to back up 50% of the mean daily heat demand in January. The efficiencies in (4) are chosen as $\beta_s = \beta_1 = \beta_2 = 0.9$ and the loss parameter in (16) is set to $\gamma = 0.75$.

Furthermore, we consider a two stage tariff structure with high prices during the day and low prices otherwise. To simplify notation, let us introduce two operation periods that correspond to operation by day and night, respectively. Let $k \in \mathbb{N}_0$ count time steps, M denote the number of sampling points in a period (24 hours) and mod be the modulo operator. With the normalized time step

$$\Delta t = \frac{24h}{M},$$

we can define sets for operation by day and night as

$$\boldsymbol{\mathcal{T}}^I = \{k \in \mathbb{N}_0 | \, (k \bmod M)\, \Delta t \in (6h, 22h]\},$$
$$\boldsymbol{\mathcal{T}}^{II} = \{k \in \mathbb{N}_0 | \, (k \bmod M)\, \Delta t \notin (6h, 22h]\}.$$

We consider a two-story single family building based on the reference building called *SFH60* developed in Task 32 of the International Energy Agency [15, pp.5-7] as consumption subsystem. The building model is derived with openBuild [6]. The building has an annual heat demand of 60 $\frac{kWh}{m^2 a}$. It is divided into 4 occupied zones and 1 attic zone. The occupied zones have an area of 160 m^2. The dimensions of the building model are $\xi(k) \in \mathbb{R}^{144}$, $\nu(k) \in \mathbb{R}^4$ and $\zeta(k) \in \mathbb{R}^{80}$.

The zones have to be operated within the comfort windows listed in Table I. The ground floor zones Z_1 and Z_2 are operated with set-point tracking during period $\boldsymbol{\mathcal{T}}^I$, representing a stronger comfort requirement for a subset of the occupied zones. We choose $T^{set}_{Z,1}(k) = 21°\mathrm{C}$, $T^{set}_{Z,2}(k) = 20°\mathrm{C}$ for all $k \in \mathcal{T}^I$. The heat gains originating from external conditions, occupancy and electrical appliances are calculated by openBuild [6] and collected in $\zeta(k)$. Weather data is taken from a test reference year supplied by the German weather forecast provider *DWD* [16]. An occupancy profile based on a family of four is chosen according to the building research benchmark described in [17, pp.4-7].

TABLE I: Zone comfort windows in °C

Period	$\mathcal{T}^I$		$\mathcal{T}^{II}$	
Zone	min	max	min	max
Z_1	19.5°C	22°C	17.5°C	22.5°C
Z_2	19.5°C	22°C	17.5°C	22.5°C
Z_3	19.5°C	22°C	17.5°C	22.5°C
Z_4	18.5°C	24°C	17.5°C	25°C
Z_A	10°C	27°C	10°C	27°C

B. Specification of scalar costs

Various requirements in building heating control dictate the choice of scalar costs $c_l(k), l \in \mathcal{L}$. We choose $c_{g,1}(k) = 1000$, $c_{g,2}(k) = 5000$, $c_s(k) = 0.1$, $c_{Z,j}(k) = 10, j = 1, \ldots, 4$, $c_{set,1}(k) = 1$, $c_{set,2}(k) = 0.5$ and $c_{set,j}(k) = 0, j = 3, 4$ for all $k \in \mathcal{T}^I$. Choosing $c_{g,1}(k) < c_{g,2}(k)$ for all (k) puts higher cost on auxiliary heat generated and causes the heat pump to be used whenever possible. The low cost on $c_s(k)$ describes the preference of using stored heat during $\mathcal{T}^I$. The choice of $c_{set,1}(k) = 1$ and $c_{set,2}(k) = 0.5$ represents the differing significance of regulating these two zones to the set point. The costs related to heat generators and set point tracking of zone temperatures differ among periods $\mathcal{T}^I$ and $\mathcal{T}^{II}$ as follows. Since both heat generators consume electricity and since electricity is cheaper at night than during the day, it holds

$$c_{g,j_{HG}}(\tilde{k}) < c_{g,j_{HG}}(k) \; \forall \left(\tilde{k}, k\right) \in \mathcal{T}^{II} \times \mathcal{T}^I.$$

As it is also not required to track a set point at night, we further choose $c_{set,j}(k) = 0, j = 1, \ldots, 4$ for all $k \in \mathcal{T}^{II}$. The scalar costs related to storage discharging $c_s(k)$ and to the heat flows into the zones $c_{Z,j}(k)$ are kept constant.

An additional challenge in weight tuning is that the dynamics of the building strongly depends on the measured disturbances $\mathbf{d}(k)$. To cope with uncertainties in the predictions and their increase along the prediction horizon N, we decrease the influence of more distant prediction steps on the cost function (15). In particular, we choose

$$c_l(k+i) = \begin{cases} c_l(k+i), & \text{if } i \leq \frac{N}{2} \\ 0.1 \cdot c_l(k+i), & \text{if } i \leq \frac{3N}{4} \\ 0.01 \cdot c_l(k+i), & \text{if } i > \frac{3N}{4} \end{cases}, \forall l \in \mathcal{L}. \quad (22)$$

Without this modification, the controller overvalues the impact of far distant weather predictions, which in general are less accurate than predictions in the near future.

C. Yesterday-based disturbance predictions

We first run all simulations of the controlled system under the assumption of perfect knowledge of the disturbances. All results obtained under this assumption are referred to as reference results, because they provide an upper bound on the controller performance. We compare the reference solution to results obtained under the assumption that the disturbances of the previous 24 hours are reasonable predictions for the disturbances in the following 24 hours. This essentially is equivalent to the assumption that the occupant's behavior and the weather change only slowly between two consecutive days. We refer to this choice with the term yesterday-based predictions.

V. Simulation results

A. Control performance

We run simulations with a time-step of $0.25h$ and a horizon of 24 hours, i.e. $N = 96$, and assume noise-free full state measurements. Results for one arbitrary week of operation during the heating period, i.e. the period between October and April, are shown in Figs. 2 to 5. Yellow and blue background refer to $\mathcal{T}^I$ and $\mathcal{T}^{II}$, respectively.

Fig. 2 shows the zone temperatures of the occupied zones and their lower and upper bounds. The results for yesterday-based predictions and reference results obtained for known disturbances are shown with continuous and dashed lines, respectively. The common bounds of zones 1 and 2 in Fig. 2a are depicted as purple dotted lines. In Fig. 2b, the blue, green and turquoise dotted lines represent the bounds, where turquoise represents the common upper bound of zones 3 and 4. The set points in Fig. 2a are depicted with blue and red dotted lines. We observe that the occupied zones are always operated within the comfort windows when the predictions are perfect. Due to larger difference in the behavior of the occupants between week and weekend, small violations occur on transient days when yesterday-based predictions are used. For example, see day 6 in Fig. 2a, where the controller underestimates the internal gains and thus the zone temperatures are regulated above the set point. In both cases, the temperature in zone 1 is in general held close to the set point during the day and drops to a certain level at night. For zone 2, we observe a similar behavior, while there is a larger distance to the set point, which is consistent with the relation of the costs $c_{set,2}(k) < c_{set,1}(k)$. Zones 3 and 4 are usually operated closer to their lower bounds due to the objective of minimizing the operational cost, see Fig. 2b. Please note that there are only small violations in case of yesterday-based predictions and no violations for reference results obtained for known disturbances.

We show the results for the heat flows and the state of charge for the case with yesterday-based predictions only. The supplied heat is depicted in Fig. 3 and shows that little to no heat has to be supplied to zones 3 and 4, which can freely be operated in the comfort windows. This shows the ability of the controller to exploit the comfort windows to reduce energy costs. The set point tracking requirement leads to an increase in heat supplied to the ground floor zones, which, as a side effect, also reduces the energy demand of the first floor. We further note a small heat supply into the building during night operation, which increases as period

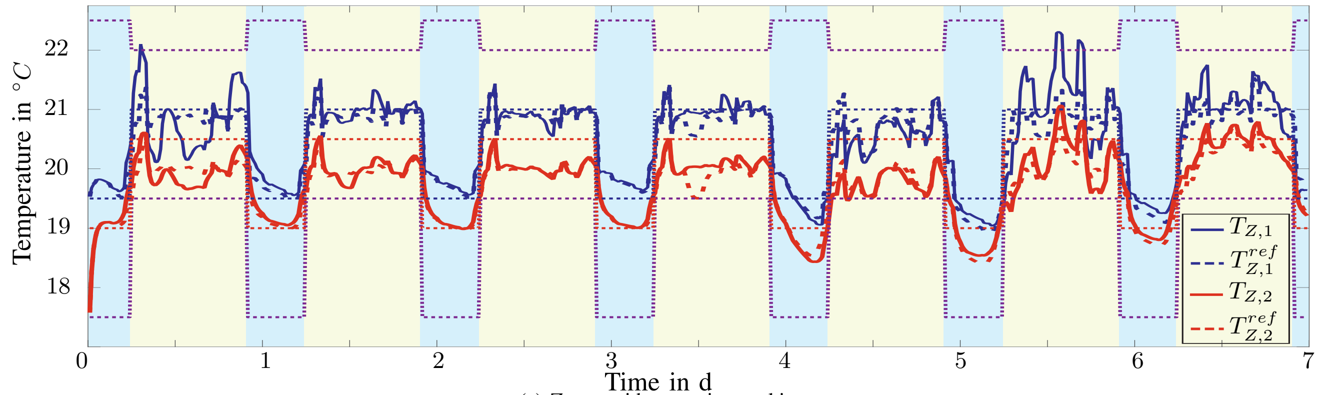

(a) Zones with set point tracking

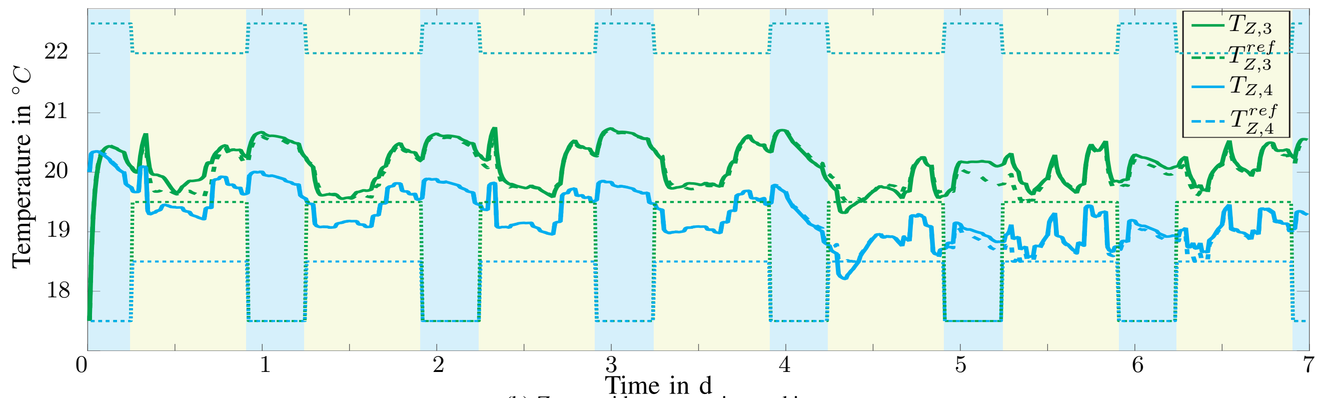

(b) Zones without set point tracking

Fig. 2: Temperatures in building zones

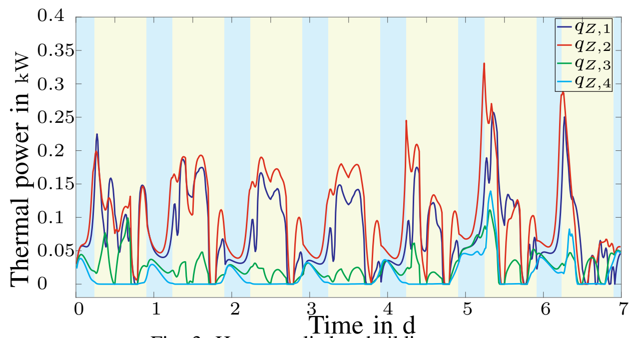

Fig. 3: Heat supplied to building zones

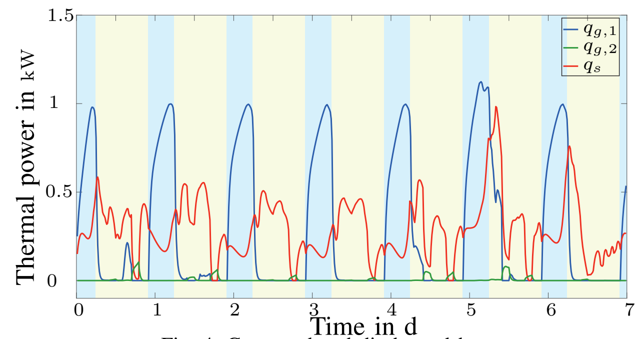

Fig. 4: Generated and discharged heat

$\mathcal{T}^I$ approaches. This can be explained by the actions of the heat generation system shown in Fig. 4. Supplying some heat at night is cheap compared to abrupt heating in the morning, as the heat pump is already generating heat at low cost. During $\mathcal{T}^I$, the controller manages to provide the required heat predominantly from the stored heat. The heat pump, on the other hand, can be operated primarily during period $\mathcal{T}^{II}$, when heat can be generated at lower cost. Figure 4 also reveals that the auxiliary heater only was turned on at low power during scheduled blocking times. However, it is essential to consider it as backup solution for unexpected and unpredictable off times of the heat pump or rapid changes in temperature that may occur in practice. Figure 5 shows that the storage is mainly charged at night and discharged during the day. Due to this anticipatory operation of the storage, less than 25% of the heat had to be generated during the day, while more than 65% of the heat was demanded in this period.

B. Statistical analysis

We further analyzed the control performance for both the reference case and the case with yesterday-based disturbance predictions by simulating a whole heating season. We provide means of the weekly absolute heat load in the system in Table II for the reference case. In the table, Q_l denotes the amount of heat generated and distributed with heat flows $q_l(k), l \in \mathcal{L}$. We investigate the performance of the controller with yesterday-based predictions by comparing it to the reference case. The mean weekly differences in energy generation and consumption are listed in Table III and given relative to the results presented in Table II. In general, we see that the amount of heat that the system needs to deliver is quite similar. The change in periods of heat generation, however, leads to a slight increase in operational

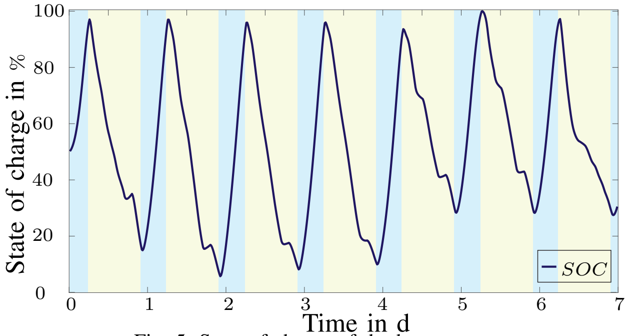

Fig. 5: State of charge of the heat storage

TABLE II: Mean absolute heat load in kWh

Zone \ Period	Overall	$\mathcal{T}^{\mathcal{I}}$	$\mathcal{T}^{\mathcal{II}}$
$Q_{g,1}$	232 kWh	49 kWh	183 kWh
$Q_{g,2}$	28 kWh	20 kWh	8 kWh
Q_s	248 kWh	163 kWh	85 kWh
$Q_{Z,1}$	52 kWh	38 kWh	14 kWh
$Q_{Z,2}$	74 kWh	53 kWh	21 kWh
$Q_{Z,3}$	26 kWh	13 kWh	13 kWh
$Q_{Z,4}$	21 kWh	9 kWh	12 kWh

cost. The spike of 82.3% for $Q_{g,2}$ in period $\mathcal{T}^{\mathcal{II}}$ can be neglected in the performance rating, as the corresponding absolute value in Table II is small compared to the overall supplied heat.

We list the mean hours with constraint violations for both cases in Table IV. Note that there were no constraint violations in the reference case.

TABLE III: Relative difference in heat flows

Zone \ Period	Overall	$\mathcal{T}^{\mathcal{I}}$	$\mathcal{T}^{\mathcal{II}}$
$Q_{g,1}$	4.2 %	21.3 %	3.0 %
$Q_{g,2}$	11.2 %	11.3 %	82.3 %
Q_s	9.3 %	7.4 %	13.1 %
$Q_{Z,1}$	5.9 %	4,5 %	10.1 %
$Q_{Z,2}$	3.2 %	1.9 %	6.9 %
$Q_{Z,3}$	11.8 %	8.6 %	16.6 %
$Q_{Z,4}$	10.4 %	2 %	16.2 %

TABLE IV: Weekly mean comfort violations in hours

Type	$\mathcal{T}^{\mathcal{I}}$		$\mathcal{T}^{\mathcal{II}}$	
Zone	low	up	low	up
Z_1	1.6 h	0 h	0 h	0 h
Z_2	0 h	3.3 h	0 h	0 h
Z_3	0 h	3.6 h	0.4 h	0 h
Z_4	0 h	2.8 h	0 h	0 h

The small numbers prove that the comfort is rarely affected, but also indicate that the system is operated more closely to the bounds. We claim that the controller is capable of mostly maintaining the low energy consumption without violating comfort windows.

VI. Conclusions

We proposed and analyzed a predictive control approach for heat flow control in domestic buildings. The continuously varying ambient conditions of the building were collected as operational constraints. The objective consisted in maintaining thermal comfort while operating the heating system in an economic fashion. The proposed approach performs well even if data of the previous day is used to predict the disturbances of the upcoming day. We conclude the approach is in general well suited even if only historical data on disturbances is available.

References

[1] L. Pérez-Lombard, J. Ortiz, and C. Pout, "A review on buildings energy consumption information," *Energy and Buildings*, vol. 40, no. 3, pp. 394 – 398, 2008.

[2] M. Fiorentini, J. Wall, Z. Ma, J. H. Braslavsky, and P. Cooper, "Hybrid model predictive control of a residential HVAC system with on-site thermal energy generation and storage," *Applied Energy*, vol. 187, no. Supplement C, pp. 465 – 479, 2017.

[3] Y. Wang, J. Kuckelkorn, and Y. Liu, "A state of art review on methodologies for control strategies in low energy buildings in the period from 2006 to 2016," vol. 147, May 2017.

[4] D. Sturzenegger, D. Gyalistras, V. Semeraro, M. Morari, and R. S. Smith, "BRCM matlab toolbox: Model generation for model predictive building control," in *American Control Conference (ACC), 2014*. IEEE, 2014, pp. 1063–1069.

[5] D. B. Crawley, C. O. Pedersen, L. K. Lawrie, and F. C. Winkelmann, "EnergyPlus: energy simulation program," *ASHRAE journal*, vol. 42, no. 4, pp. 49–56, 2000.

[6] T. T. Gorecki, F. A. Qureshi, and C. N. Jones, "OpenBuild: An integrated simulation environment for building control," in *2015 IEEE Conference on Control Applications (CCA)*, September 2015, pp. 1522–1527.

[7] V. Chandan and A. G. Alleyne, "Decentralized predictive thermal control for buildings," *Journal of Process Control*, vol. 24, no. 6, pp. 820 – 835, 2014.

[8] R. Halvgaard, N. K. Poulsen, H. Madsen, and J. B. Jørgensen, "Economic model predictive control for building climate control in a smart grid," in *Innovative Smart Grid Technologies (ISGT), 2012 IEEE PES*. IEEE, 2012, pp. 1–6.

[9] F. Oldewurtel, D. Sturzenegger, and M. Morari, "Importance of occupancy information for building climate control," *Applied Energy*, vol. 101, pp. 521 – 532, 2013.

[10] M. Maasoumy, M. Razmara, M. Shahbakhti, and A. S. Vincentelli, "Handling model uncertainty in model predictive control for energy efficient buildings," *Energy and Buildings*, vol. 77, pp. 377 – 392, 2014.

[11] Y. Löhr and M. Mönnigmann, "Domestic heat generation and distribution with time-variant receding horizon control," *IFAC-PapersOnLine*, vol. 50, no. 1, pp. 4191 – 4196, 2017.

[12] J. M. Maciejowski, *Predictive control: with constraints*. Englewood Cliffs, NJ: Prentice Hall, 2002.

[13] W. Grote, "Ein Beitrag zur modellbasierten Regelung von Entnahmedampfturbinen," Ph.D. dissertation, Ruhr-Universität Bochum, 2009, Schriftenreihe, Lehrstuhl für Regelungssysteme und Steuerungstechnik.

[14] H. Cheung and J. E. Braun, "Performance mapping for variable-speed ductless heat pump systems in heating and defrost operation," *HVAC&R Research*, vol. 20, no. 5, pp. 545–558, 2014.

[15] R. Heimrath and M. Haller, "The reference heating system, the template solar system of task 32," International Energy Agency, Tech. Rep., May 2007.

[16] DWD Climate Data Center (CDC), "Ortsgenaue Testreferenzjahre (TRY) von Deutschland für mittlere und extreme Witterungsverhältnisse," 2010.

[17] F. Omar and S. T. Bushby, "Simulating occupancy in the NIST net-zero energy residential test facility," NIST National Insttitute of Standards and Technology, Tech. Rep., November 2013.